Carbon Dioxide Reforming of Methane in Kilohertz Spark-Discharge Plasma at Atmospheric Pressure

Xiao-Song Li, Bin Zhu, Chuan Shi, Yong Xu, and Ai-Min Zhu
Laboratory of Plasma Physical Chemistry, Dalian University of Technology, Dalian 116024, China

DOI 10.1002/aic.12472
Published online November 29, 2010 in Wiley Online Library (wileyonlinelibrary.com).

The spark-discharge plasma, generated between tubular and rotary-disc electrodes using a sine-wave high voltage with 5 kHz frequency, was explored for CO_2 reforming of CH_4. Based upon the investigation on the effects of specific energy input and CO_2/CH_4 ratio, the energy costs (EC) and fuel-production efficiencies (η) at various CO_2/CH_4 ratios (r) in the same conversion range were compared and accordingly their sequences were given: EC_{CH_4} (r = 0.5) and EC_{CO_2} (r = 3) are the lowest; η(r = 0.5) is the highest. Compared with other nonthermal discharge techniques, the kilohertz spark discharge exhibits low EC and high fuel-production efficiency, especially at high total-carbon conversions. Preliminary investigation on partial oxidation and CO_2 mixed reforming at $(O_2 + CO_2)/CH_4 = 0.5$ exhibited high H_2/CO ratio (nearly 2) and low total-carbon EC (0.59–0.96 MJ/mol, 58–77% of total-carbon conversion, and $O_2/(CO_2 + O_2) = 0.8$). © 2010 American Institute of Chemical Engineers *AIChE J,* 57: 2854–2860, 2011

Keywords: carbon dioxide, reforming, methane, plasma, spark discharge

Introduction

The reaction of carbon dioxide reforming (CDR) of methane to produce synthesis gas (syngas) has currently attracted considerable interests for natural gas and biomethane conversions and for environmental control.[1] However, there exist some major drawbacks for the catalytic CDR reaction: the high temperature required and the rapid deactivation due to coke and sulfur poisoning. A desirable alternative is the use of nonthermal plasma, in which the collision of energetic electrons with gas molecules can produce radicals to induce chemical reactions, resulting in very high methane conversion at relatively low temperature in comparison with the conventional catalytic process.

CDR of methane via nonthermal plasmas has been extensively studied by using various discharge techniques, such as corona/spark discharge,[2–6] microwave discharge,[7] dielectric barrier discharge (DBD),[8–14] and gliding arc discharge.[15] Generally, gliding arc discharge showed lower energy cost (EC) than corona discharge, microwave discharge, or DBD.[16] However, the conversions of CO_2 and CH_4 in gliding arc discharges are relatively low. For practical applications, low EC at high reactant conversions should be required. Additionally, to meet the demand of methanol synthesis from syngas with high H_2/CO ratio up to 2, CO_2/CH_4 ratio less than 1 in feed is required. However, the low CO_2/CH_4 ratio results in the rapid deterioration in the discharge derived from carbonaceous deposition.[17] In our previous work,[18] using a tubular high-voltage electrode and a rotary-disc ground electrode, the deterioration problem in the discharge was solved successfully and stable kilohertz spark discharges in pure CH_4 were achieved. Moreover, high conversion of methane and low EC for converting CH_4 were reported in the kilohertz spark-discharge plasma. Therefore, the kilohertz spark-discharge plasma was explored for CDR of CH_4 in this work. EC and fuel-production efficiency vs.

Correspondence concerning this article should be addressed to A.-M. Zhu at amzhu@dlut.edu.cn.

total-carbon conversion were particularly investigated and compared with those in other nonthermal discharges. Preliminary investigation was also made for partial oxidation (POX) and CO_2 mixed reforming in this plasma.

Experimental

The spark discharge reactor consisted of a rotary stainless-steel disc (30 mm of diameter and 3 mm of thickness) as the ground electrode and a stainless steel tube (1-mm internal diameter × 2-mm external diameter) as the high-voltage electrode.[18] The gap distance between the two electrodes was 6 mm. The two electrodes were placed in a quartz tube (100-mm internal diameter × 100-mm height). The reactor was cooled with water at the top and bottom covers of the quartz tube. A thermocouple lies at the center of the reactor to monitor the reactor temperature. The feed gas was introduced into the reactor from the tubular electrode. The power supply source can provide a sine-wave high voltage with a frequency of 5 kHz. The voltage and current waveforms were measured with an oscilloscope (TDS2024B, Tektronix) via a voltage probe (P6015A, Tektronix) and a sampling resistor (10 Ω), respectively.[18] The total input power was measured using a wattmeter in the primary side of the transformer.

Methane (99.99%) and carbon dioxide (99.99%), controlled by mass flow controllers (Sevenstar Electronics, China), were used as the feed gas to the reactor. All experiments were performed at atmospheric pressure. N_2 (99.999%) was used as an internal standard for analysis and introduced into the effluent gas from the plasma reactor to avoid conversion of N_2 in the plasma.[19,20] The effluent gas flowed through an ice-water-cold trap and then was sampled for online analysis. The first gas chromatograph (Agilent 1790 T), equipped with a thermal conductivity detector (TCD) using H_2 as the carrier gas, was used to detect N_2, CO, CH_4, and CO_2 with a TDX-01 column (2-mm I. D. × 1.5-m length). For POX and CO_2 mixed reforming experiments, a 5A molecular sieve column (2-mm I. D. × 1-m length) was added to detect N_2, O_2, and CH_4 using the first gas chromatograph. Hydrocarbon products and hydrogen were on-line analyzed by the second gas chromatograph (Agilent 6890 N), equipped with a flame ionization detector and TCD using N_2 as the carrier gas with a Porapak-N column (2-mm I. D. × 3-m length) and a carbon molecular sieve of 601 column (2-mm I. D. × 1-m length), respectively.

The conversions of CH_4 (X_{CH_4}), CO_2 (X_{CH_2}), O_2 (X_{O_2}), and total carbon (X_{TC}) and the selectivities of CO (S_{CO}) and hydrocarbons (S_{CH_xHy}) were evaluated using the internal standard analyzing method. In terms of the flow rate of N_2 (F_{N_4}) used as internal standard and the molar concentration of N_2 (C_{N2}^{out}) in the effluent gas given by the first gas chromatograph, the total effluent gas flow rate (F^{out}) can be expressed by the following equation

$$F^{out} = F_{N_2} \Big/ C_{N_2}^{out} \tag{E1}$$

Then X_{CH_4}, X_{CO_2}, X_{O_2}, and X_{TC} were calculated from the following equations

$$X_{CH_4} = 1 - F^{out} \cdot C_{CH_4}^{out} \Big/ F_{CH_4}^{in} \tag{E2}$$

$$X_{CO_2} = 1 - F^{out} \cdot C_{CO_2}^{out} \Big/ F_{CO_2}^{in} \tag{E3}$$

$$X_{O_2} = 1 - F^{out} \cdot C_{O_2}^{out} \Big/ F_{O_2}^{in} \tag{E4}$$

$$X_{TC} = (F_{CH_4}^{in} \cdot X_{CH_4} + F_{CO_2}^{in} \cdot X_{CO_2}) \Big/ (F_{CH_4}^{in} + F_{CO_2}^{in}) \tag{E5}$$

where F_{CH4}^{in}, F_{CH4}^{out}, F_{CO2}^{in}, F_{CO2}^{out}, F_{O2}^{in}, and F_{O2}^{out} represent the flow rates of CH_4, CO_2, and O_2 at the inlet and outlet of the reactor, respectively; C_{CH4}^{out}, C_{CO2}^{out}, and C_{O2}^{out}, given by the first gas chromatograph, represent the molar concentrations of CH_4, CO_2, and O_2 in the effluent gas, respectively.

The selectivities of CO (S_{CO}) and hydrocarbons (S_{C_xHy}) were calculated from the following equations

$$S_{CO} = F^{out} \cdot C_{CO}^{out} \Big/ (F_{CH_4}^{in} \cdot X_{CH_4} + F_{CO_2}^{in} \cdot X_{CO_2}) \tag{E6}$$

$$S_{C_xH_y} = x \cdot F^{out} \cdot C_{C_xH_y}^{out} \Big/ (F_{CH_4}^{in} \cdot X_{CH_4} + F_{CO_2}^{in} \cdot X_{CO_2}) \tag{E7}$$

Here, x and y represent carbon-atom number and hydrogen-atom number in a molecule of hydrocarbon product, respectively. C_{CO}^{out} and C_{CxHy}^{out}, given by the first and second gas chromatograph, represent the molar concentrations of CO and hydrocarbons in the effluent gas, respectively. Carbon balance (B_C) was defined as the following equation

$$B_C = F^{out} \cdot (x \cdot C_{C_xH_y}^{out} + C_{CH_4}^{out} + C_{CO_2}^{out} + C_{CO}^{out}) \Big/ (F_{CH_4}^{in} + F_{CO_2}^{in}) \tag{E8}$$

Hydrogen selectivity (S_{H_2}) was calculated from the following equation

$$S_{H_2} = 0.5 \cdot F^{out} \cdot C_{H_2}^{out} \Big/ (F_{CH_4}^{in} \cdot X_{CH_4}) \tag{E9}$$

Here, C_{H2}^{out}, given by the second gas chromatograph using the external standard analyzing method, represents the molar concentration of H_2 in the effluent gas. H_2O selectivity (S_{H_2O}) based upon hydrogen atoms was calculated from E10

$$S_{H_2O} = 0.5 \cdot F_{H_2O} \Big/ (F_{CH_4}^{in} \cdot X_{CH_4}) \tag{E10}$$

where F_{H_2O} was calculated from E11 assuming the total amount of O atoms in CO_2 converted is equal to that in CO and H_2O produced.

$$F_{H_2O} = 2F_{CO_2}^{in} \cdot X_{CO_2} - F^{out} \cdot C_{CO}^{out} \tag{E11}$$

The specific energy input (SEI, kJ/dm^3) in this work was defined as the total input power (P_{input}, W) divided by the total flow rate ($F_{CH_4}^{in} + F_{CO_2}^{in}$, standard cubic centimeters per minute, SCCM).

$$SEI = 60 \cdot P_{input} \Big/ (F_{CH_4}^{in} + F_{CO_2}^{in}) \tag{E12}$$

The ECs (MJ/mol) for converting total carbon (EC_{TC}), methane (EC_{CH_4}), and carbon dioxide (EC_{CO_2}) were calculated as follows

$$EC_{TC} = 1.344 \cdot P_{input} \Big/ (F^{in}_{CO_2} \cdot X_{CO_2} + F^{in}_{CH_4} \cdot X_{CH_4}) \quad \text{(E13)}$$

$$EC_{CH_4} = 1.344 \cdot P_{input} \Big/ (F^{in}_{CH_4} \cdot X_{CH_4}) \quad \text{(E14)}$$

$$EC_{CO_2} = 1.344 \cdot P_{input} \Big/ (F^{in}_{CO_2} \cdot X_{CO_2}) \quad \text{(E15)}$$

The fuel-production efficiency was defined as the following equation according to Ref. 21

$$\eta = F^{out} \cdot (C^{out}_{C_xH_y} \cdot LHV_{C_xH_y} + C^{out}_{CO} \cdot HV_{CO} + C^{out}_{H_2} \cdot LHV_{H_2}) \Big/ (P_{input} + F^{in}_{CH_4} \cdot X_{CH_4} \cdot LHV_{CH_4}) \quad \text{(E16)}$$

where LHV is the lower heating value of a fuel, excluding the heat given by condensing the water vapor.

Results and Discussion

Effect of SEI

Figure 1 shows effects of SEI on conversions, H_2/CO ratio, selectivities, and carbon balance at 150 SCCM of total flow rate and $CO_2/CH_4 = 0.5$. Increasing SEI from 12 to 20 kJ/dm^3, the conversions of CH_4, CO_2, and total carbon increased from 48%, 36%, and 44% to 60%, 50%, and 57%, respectively (Figure 1a). This demonstrates that SEI has a powerful and positive effect on CH_4, CO_2, and total-carbon conversions. Additionally, H_2/CO ratio decreased slightly from 2.3 to 1.9 with the increase of SEI (Figure 1a). According to the CDR reaction (R1)

$$CO_2 + CH_4 \rightarrow 2CO + 2H_2 \quad \text{(R1)}$$

the H_2/CO ratio should be equal to 1. Why H_2/CO ratio at $CO_2/CH_4 = 0.5$ was more than 1.8? The reason is that methane dehydrogenated-coupling reaction (R2) simultaneously occurred especially in the presence of excess methane.

$$CH_4 \rightarrow 1/2\,C_2H_2 + 3/2\,H_2 \quad \text{(R2)}$$

In the case of $CO_2/CH_4 = 0.5$, C_2H_2 selectivities reached 48–42% at 44–57% of total-carbon conversions. Moreover, H_2 and CO selectivities attained 61–68% and 38–53%, respectively. This implies that product selectivities are weakly affected by SEI. The sum of selectivities to other carbon-containing products (including C_2H_6, C_2H_4, and C_3—C_6 hydrocarbons) were 3–8%. Carbon balance closely approached 100%.

Effect of CO_2/CH_4 ratio

CO_2/CH_4 ratio has an intense effect on the reaction of CDR with methane. As shown in Figure 2a, with increasing CO_2/CH_4 ratio from 0.5 to 4, methane conversion increased monotonically from 59% to 82%, whereas CO_2 conversion increased to the maximum (55%) at $CO_2/CH_4 = 1.5$ and then turned to decrease. For a plasma reaction, increasing concentration of a reactant generally lowers conversion of the reactant, such as

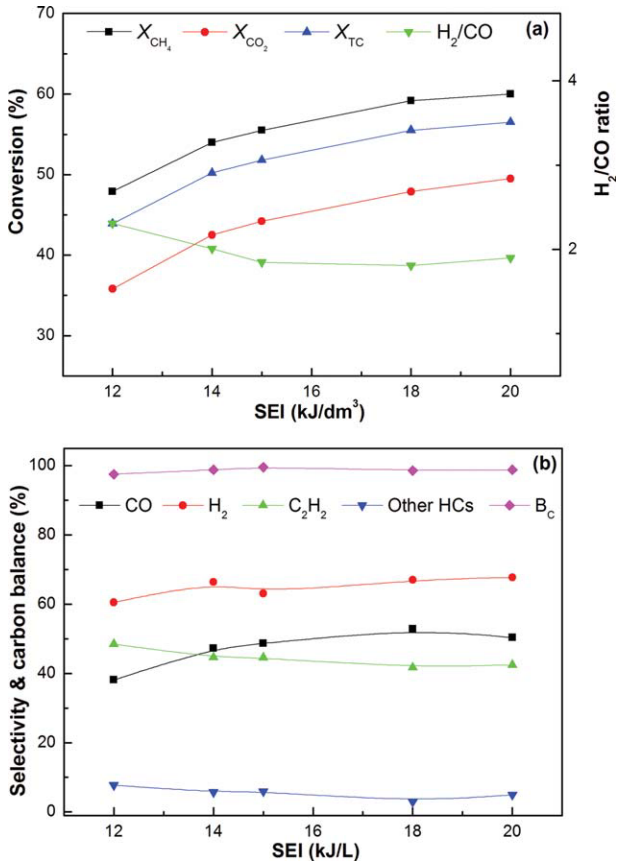

Figure 1. Effect of SEI on (a) conversions of CH_4, CO_2, and total carbon and H_2/CO ratio, and (b) selectivities of H_2, CO, and C_2H_2 and carbon balance (total flow rate = 150 SCCM, $CO_2/CH_4 = 0.5$).

[Color figure can be viewed in the online issue, which is available at wileyonlinelibrary.com.]

the variation of methane conversion vs. CO_2/CH_4 ratio in this case. According to the general rule, CO_2 conversion should decrease with the increase in CO_2/CH_4 ratio. But, why did the variation of CO_2 conversion not follow this rule in the range of $CO_2/CH_4 < 1.5$? The answer can be found in the evolution of R1 in competition with R2. In the range of $CO_2/CH_4 < 1.5$, with increasing CO_2/CH_4 ratio, R1 became more and more predominant over R2. Consequently, CO_2 conversion gradually increased with CO_2/CH_4 ratio and finally reached the maximum. The variation of C_2H_2 selectivity, as shown in Figure 2b, can reflect the evolution of the two competitive reactions with CO_2/CH_4 ratio. For example, C_2H_2 selectivity was 42% at $CO_2/CH_4 = 0.5$ and decreased to 9% at $CO_2/CH_4 = 1.5$. When CO_2/CH_4 ratio increased to more than 1.5, R2 was negligible and CO_2 conversion varied with CO_2/CH_4 ratio by the general rule. The profile of total-carbon conversion vs. CO_2/CH_4 ratio is similar to that of CO_2 conversion. At $CO_2/CH_4 = 1.5$ and SEI = 18 kJ/dm^3, the total-carbon conversion reached a maximum of 59%.

From Figure 2a, it can be easily seen that CH_4 conversions are always higher than CO_2 conversions over a whole range of CO_2/CH_4 ratio. The density functional theory study confirmed that the dissociation of CH_4 and CO_2 is the main obstacle.[22] Therefore, it can be explained from the point of

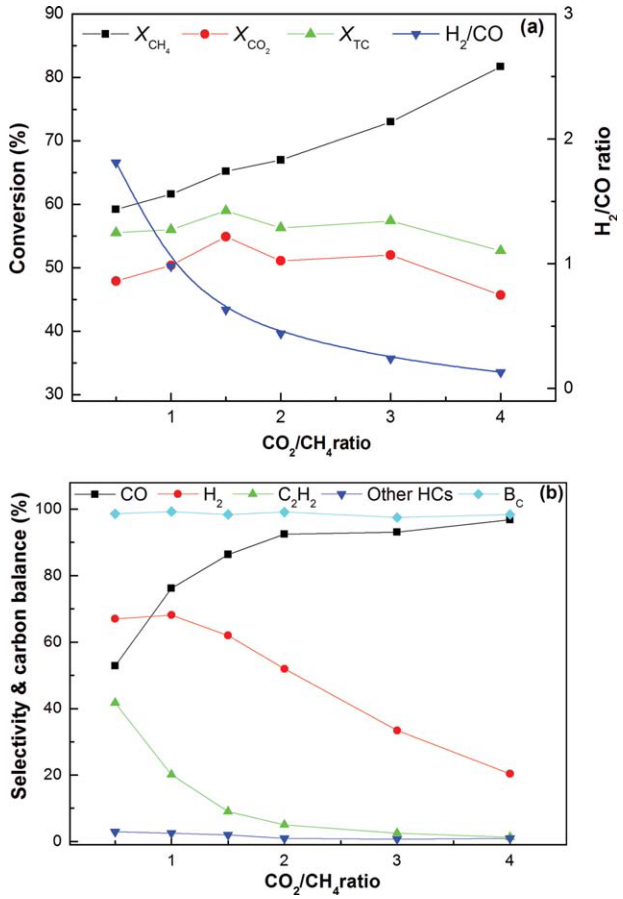

Figure 2. Effect of CO_2/CH_4 ratio on (a) conversions of CH_4, CO_2, and total carbon and H_2/CO ratio, and (b) selectivities of H_2, CO, and C_2H_2 and carbon balance (total flow rate = 150 SCCM, SEI = 18 kJ/dm^3).

[Color figure can be viewed in the online issue, which is available at wileyonlinelibrary.com.]

view of bond energy. The O=CO bond energy in CO_2 molecule is 532 kJ/mol larger than CH_3—H bond energy (439 kJ/mol) in CH_4 molecule. Additionally, at high CO_2/CH_4 ratios, the reaction of CO_2 to CO conversion was counteracted by R3,[23] R4,[24] and R5[25]

$$CO + OH \rightarrow CO_2 + H \quad k_{(T=300K)} = 1.25 \times 10^{-13} cm^3/s \quad (R3)$$

$$O(^1D) + CO \rightarrow CO_2 \quad k = 8.0 \times 10^{-11} cm^3/s \quad (R4)$$

$$CO + O + M \rightarrow CO_2 + M \quad k_{(T=300K)} = 1.11 \times 10^{-35}[M] \approx 2.7 \times 10^{-16} cm^3/s \quad (R5)$$

where $[M] \approx 2.4 \times 10^{19}$ molecule per centimeter. The ground-state $O(^3P)$ atom, metastable $O(^1D)$ atom, and OH radical were produced via reactions 6, 7,[23] and 8[26]

$$e + CO_2 \rightarrow CO + O(^3P, ^1D) + e \quad k = f(T_e) \quad (R6)$$

$$CH_4 + O \rightarrow CH_3 + OH \quad k_{(T=300K)} = 5.54 \times 10^{-18} cm^3/s \quad (R7)$$

$$CH_4 + O(^1D) \rightarrow CH_3 + OH \quad k_{(T=300K)} = 1.35 \times 10^{-10} cm^3/s \quad (R8)$$

The CO_2/CH_4 ratio exerted a stronger effect on H_2/CO ratio and H_2 selectivity than SEI did (Figures 1 and 2). For example, H_2/CO ratios at CO_2/CH_4 = 0.5 and 2 were 1.8

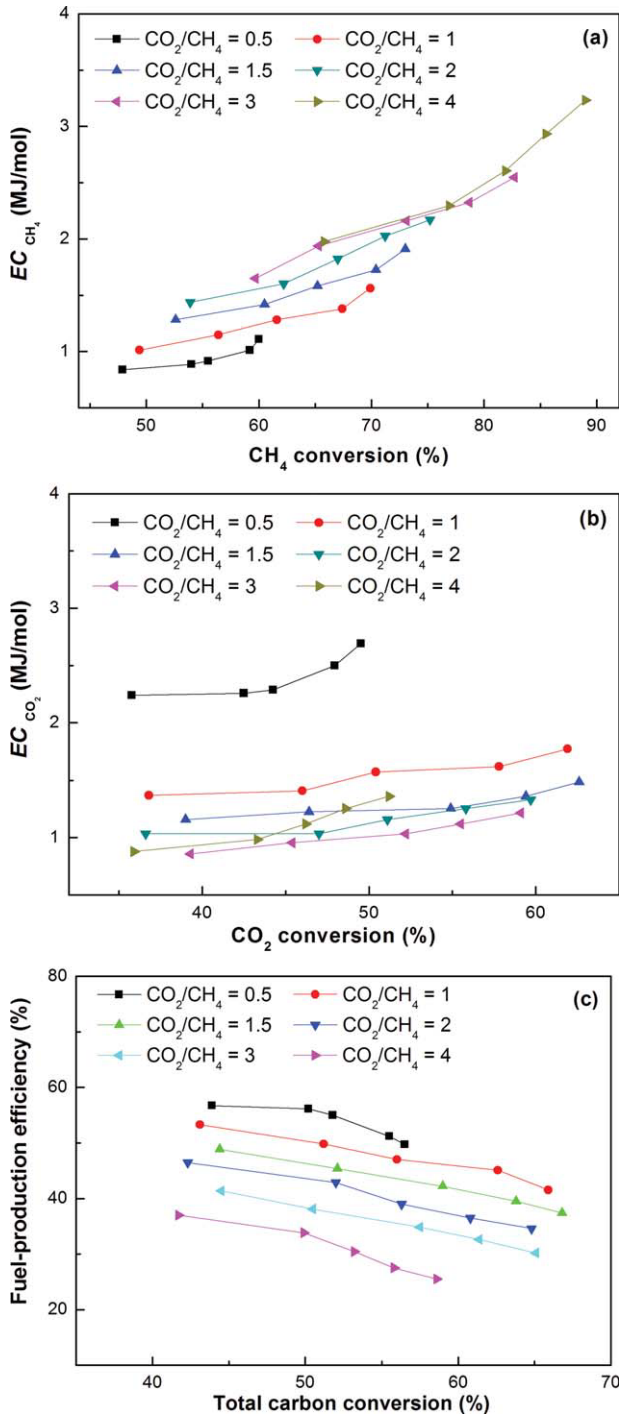

Figure 3. (a) EC_{CH_4}, (b) EC_{CO_2}, and (c) fuel-production efficiency vs. conversions at various CO_2/CH_4 ratio (total flow rate = 150 SCCM).

[Color figure can be viewed in the online issue, which is available at wileyonlinelibrary.com.]

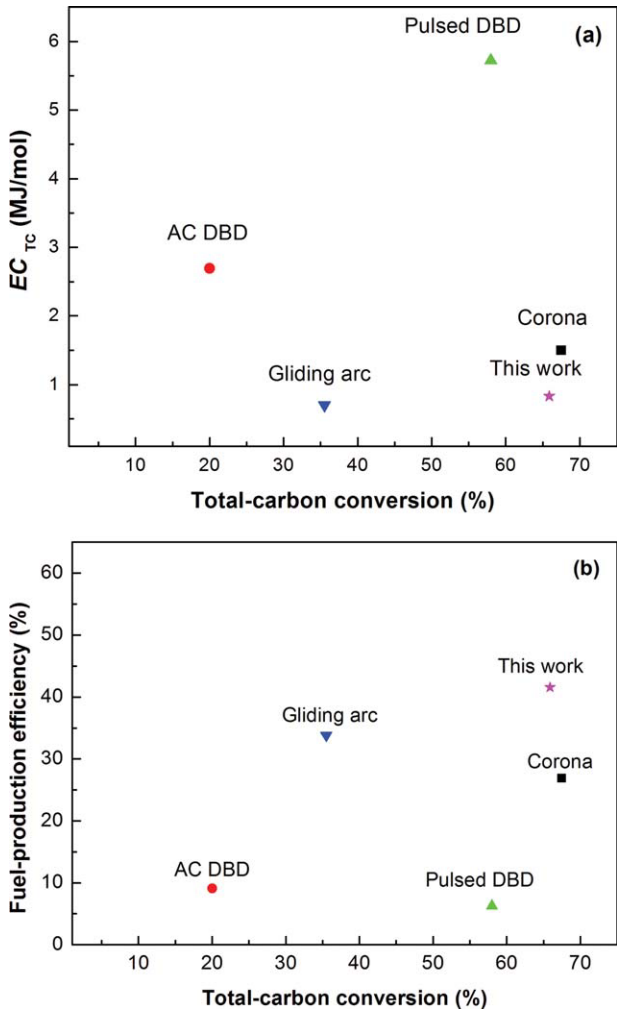

Figure 4. Maps of (a) energy cost and (b) fuel-production efficiency for typical nonthermal plasma reforming processes.

The conditions are listed in Table 1. [Color figure can be viewed in the online issue, which is available at wiley onlinelibrary.com.]

and 0.4, respectively. H_2 selectivities at $CO_2/CH_4 = 1$ and 4 were 68% and 20%, respectively (Figure 2b). The decrease in H_2 selectivity with the CO_2/CH_4 ratio can be attributed to the reaction of H_2 with CO_2 (R9)

$$CO_2 + H_2 \rightarrow CO + H_2O \qquad \text{(R9)}$$

R9 occurs to produce H_2O. H_2O selectivity was 13% at $CO_2/CH_4 = 1$ and increased to 71% at $CO_2/CH_4 = 4$ (not shown in Figure 2b). This confirms that more and more H_2O is produced with the increase in CO_2/CH_4 ratio. In the range of $CO_2/CH_4 = 0.5$–4, 98–99% of carbon balance was obtained.

EC and fuel-production efficiency

The EC for converting CH_4 and CO_2 molecules and fuel-production efficiency, as defined in Eqs. 11–14, appear to be good indicators to quantify plasma reforming systems, but their experimental results among different conditions or plasma processes can only be compared in the same range of reactant conversion.[18,27] As a result, EC and fuel-production efficiency as functions of CH_4, CO_2, and total-carbon conversions at various CO_2/CH_4 ratios are illustrated in Figures 3a, b, respectively. At the same CO_2/CH_4 ratio, EC increased and fuel-production efficiency decreased with reactant conversion. In the same range of CH_4 or CO_2 conversions, the ECs at various CO_2/CH_4 ratios (designated as r) can be grouped in the following order (except for $r = 4$)

$$\begin{aligned} &EC_{CH_4}(r = 0.5) < EC_{CH_4}(r = 1) < EC_{CH_4}(r = 1.5) \\ &\quad < EC_{CH_4}(r = 2) < EC_{CH_4}(r = 3) \\ &EC_{CO_2}(r = 0.5) \gg EC_{CO_2}(r = 1) \\ &\quad > EC_{CO_2}(r = 1.5) > EC_{CO_2}(r = 2) > EC_{CO_2}(r = 3) \end{aligned}$$

In the presence of a large excess of CO_2 ($r > 3$), the counteraction derived from R3 to R5 became very strong, thereby the amount of CO_2 conversion considerably decreased at the same SEI. Accordingly, the ECs for converting CO_2 turned to be high especially at high CO_2 conversion, e.g., at >50% CO_2 conversion, EC_{CO_2} ($r = 4$) > EC_{CO_2} ($r = 1.5$) > EC_{CO_2} ($r = 2$) > EC_{CO_2} ($r = 3$). But, for converting CH_4, the ECs at $r = 4$ were close to those at $r = 3$.

The sequence of fuel-production efficiency at various CO_2/CH_4 ratios is as follows

$$\begin{aligned} &\eta(r = 0.5) > \eta(r = 1) > \eta(r = 1.5) > \eta(r = 2) > \eta(r = 3) \\ &\quad > \eta(r = 4) \end{aligned}$$

For practical applications of plasma reforming reaction, low EC and high fuel-production efficiency should be required at high reactant conversions. Accordingly, suitable CO_2/CH_4 ratios for plasma reforming processes should be selected in the range of 0.5–1.

To make a direct comparison, EC and fuel-production efficiency for typical nonthermal plasma reforming processes[4,9,10,28] were calculated according to Eqs. 11 and 14 and mapped together with those of this work in Figure 4. The corresponding experimental conditions are summarized in Table 1. It is worth noting that because of the intense effects of CO_2/CH_4 ratio as mentioned above, all experimental data presented in Figure 4 were selected at $CO_2/CH_4 = 1$. The kilohertz spark discharge in this work exhibited low EC and high fuel-production efficiency,

Table 1. Conditions of Typical Nonthermal Plasma Reforming Processes

Discharge	Corona	AC DBD	Pulsed DBD	Gliding Arc	Spark
CO_2/CH_4	1	1	1	1	1
Feed flow rate (SCCM)	60	500	30	1000	150
SEI (kJ/dm^3)	45	24	148	11	24
Reference	4	9	10	28	This work

especially at high total-carbon conversion (>50%). EC and fuel-production efficiency in gliding arc discharges[24] are close to those in this work, but its total-carbon conversion is lower than that of this work. This efficient performance of the kilohertz spark discharge for the reforming reaction may be contributed to its moderate quench speed not only to restrain the transition to arc but also to keep relatively high plasma density for speeding up the reforming reaction rate.

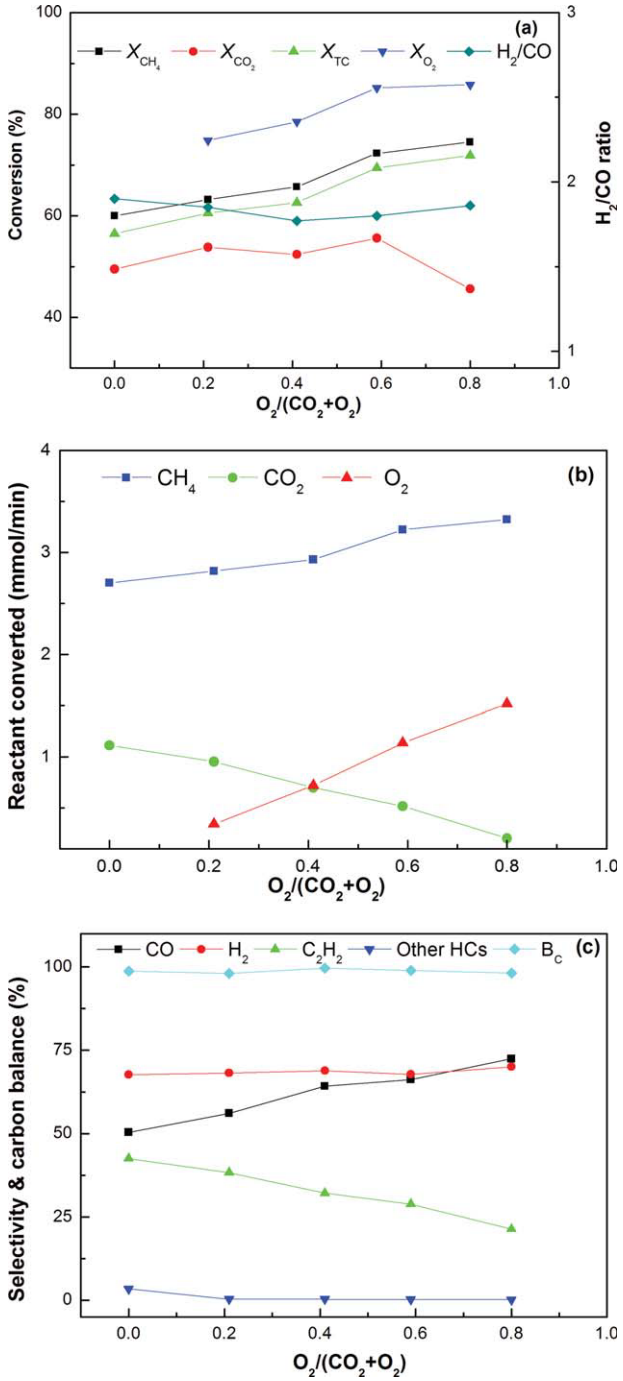

Figure 5. Effect of the $O_2/(CO_2 + O_2)$ ratio on (a) CH_4, CO_2, total carbon, and O_2 conversions and H_2/CO ratio, (b) CH_4, CO_2, and O_2 converted, and (c) H_2, CO, and C_2H_2 selectivities.

Conditions: total flow rate = 150 SCCM, $(O_2 + CO_2)/CH_4$ = 0.5, SEI = 20 kJ/dm^3. [Color figure can be viewed in the online issue, which is available at wileyonlinelibrary.com.]

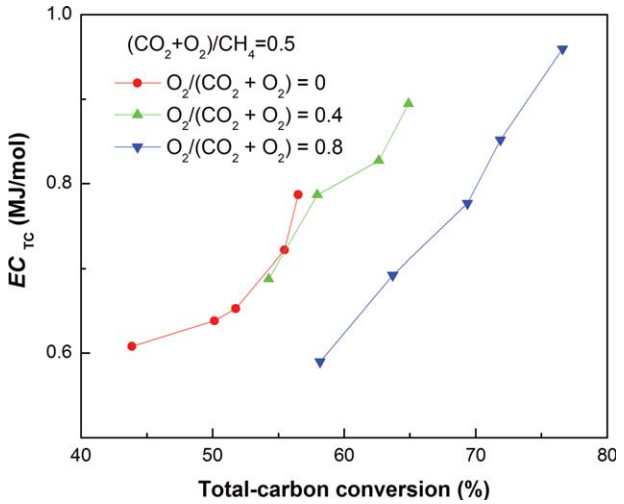

Figure 6. Energy cost vs. total-carbon conversion at various $O_2/(CO_2 + O_2)$ ratios.

Conditions: total flow rate = 150 SCCM, $(O_2 + CO_2)/CH_4$ = 0.5. [Color figure can be viewed in the online issue, which is available at wileyonlinelibrary.com.]

POX and CO_2 mixed reforming

As mentioned above (Figure 3), among all the CO_2/CH_4 ratios, the ratio of CO_2/CH_4 = 0.5 gave the highest fuel-production efficiency, but its EC (EC_{TC}) was relatively high. To lower its EC, POX and CO_2 mixed reforming were investigated at a fixed ratio of $(O_2 + CO_2)/CH_4$ = 0.5. As shown in Figure 5a, the CH_4, total-carbon, and O_2 conversions increased with $O_2/(CO_2 + O_2)$ ratio. The CO_2 conversion decreased rapidly when $O_2/(CO_2 + O_2)$ ratio increased from 0.6 to 0.8. With the increase of $O_2/(CO_2 + O_2)$ ratio, the amounts of CH_4 and O_2 converted increased, but that of CO_2 converted decreased (Figure 5b). This means, with increasing $O_2/(CO_2 + O_2)$ ratio, POX reaction became more and more dominant over CDR reaction (R1). Figure 5c shows an apparent increase in CO selectivity because of POX and CO_2 mixed reforming. H_2/CO ratio was in the range of 1.8–1.9, slightly decreasing with $O_2/(CO_2 + O_2)$ ratio. The reactor temperature slightly increased with $O_2/(CO_2 + O_2)$ ratio. At $O_2/(CO_2 + O_2)$ = 0.8, the reactor temperature rose to 337 K.

Figure 6 shows curves of EC vs. total-carbon conversion at $O_2/(CO_2 + O_2)$ = 0, 0.4, and 0.8. As expected, POX and CO_2 mixed reforming did result in lowering EC. ECs for converting total carbon at $(O_2 + CO_2)/CH_4$ = 0.5 and various $O_2/(CO_2 + O_2)$ ratios were found to be: 0.61–0.79 MJ/mol ($O_2/(CO_2 + O_2)$ = 0, X_{TC} = 44–57%), 0.69–0.90 MJ/mol ($O_2/(CO_2 + O_2)$ = 0.4, X_{TC} = 54–65%), and 0.59–0.96 MJ/mol ($O_2/(CO_2 + O_2)$ = 0.8, X_{TC} = 58–77%). It implies that EC can be further lowered by optimizing POX and CO_2 mixed reforming.

Conclusions

The kilohertz spark discharge was explored for CDR of CH_4. SEI has a powerful and positive effect on CH_4, CO_2,

and total-carbon conversions and a weak effect on product selectivities. Increasing CO_2/CH_4 ratio, methane conversion increased monotonically, whereas CO_2 conversion increased to the maximum and then turned to decrease.

In the same conversion range, the ECs and fuel-production efficiencies (η) at various CO_2/CH_4 ratios can be grouped in the following order

$$\mathrm{EC}_{\mathrm{CH_4}}(r=0.5) < \mathrm{EC}_{\mathrm{CH_4}}(r=1) < \mathrm{EC}_{\mathrm{CH_4}}(r=1.5) < \mathrm{EC}_{\mathrm{CH_4}}(r=2) < \mathrm{EC}_{\mathrm{CH_4}}(r=3)$$

$$\mathrm{EC}_{\mathrm{CO_2}}(r=0.5) \gg \mathrm{EC}_{\mathrm{CO_2}}(r=1) > \mathrm{EC}_{\mathrm{CO_2}}(r=1.5) > \mathrm{EC}_{\mathrm{CO_2}}(r=2) > \mathrm{EC}_{\mathrm{CO_2}}(r=3)$$

$$\eta(r=0.5) > \eta(r=1) > \eta(r=1.5) > \eta(r=2) > \eta(r=3) > \eta(r=4)$$

Compared with gliding arc and corona discharges and DBD, the kilohertz spark discharge exhibits low EC and high fuel-production efficiency, especially at high total-carbon conversion.

Preliminary investigation on POX and CO_2 mixed reforming at $(O_2 + CO_2)/CH_4 = 0.5$ exhibited high H_2/CO ratio (nearly 2) and low EC: $\mathrm{EC_{TC}} = 0.59$–0.96 MJ/mol ($O_2/(CO_2 + O_2) = 0.8$, $X_{\mathrm{TC}} = 58$–77%).

Acknowledgments

This work was supported by the Fundamental Research Funds for the Central Universities and the National Natural Science Foundation of China (Grant No. 10775028).

Literature Cited

1. Istadi, Amin NAS. Co-generation of synthesis gas and C_{2+} hydrocarbons from methane and carbon dioxide in a hybrid catalytic-plasma reactor: a review. *Fuel*. 2006;85:577–592.
2. Malik MA, Jiang XZ. The CO_2 reforming of natural gas in a pulsed corona discharge reactor. *Plasma Chem Plasma Process*. 1999;19: 505–512.
3. Kado S,Urasaki K,Sekine Y,Fujimoto K. Low temperature reforming of methane to synthesis gas with direct current pulse discharge method. *Chem Commun*. 2001:415–416.
4. Li MW, Tian YL,Xu GH. Characteristics of carbon dioxide reforming of methane via alternating current (AC) corona plasma reactions. *Energy Fuel*. 2007;21:2335–2339.
5. Seyed-Matin N,Jalili AH,Jenab MH,Zekordi SM,Afzali A,Rasouli C,Zamaniyan A. DC-pulsed plasma for dry reforming of methane to synthesis gas. *Plasma Chem Plasma Process*. 2010;30:333–347.
6. Ghorbanzadeh AM,Norouzi S,Mohammadi T. High energy efficiency in syngas and hydrocarbon production from dissociation of CH_4-CO_2 mixture in a non-equilibrium pulsed plasma. *J Phys D: Appl Phys*. 2005;38:3804–3811.
7. Zhang JQ,Zhang JS,Yang YJ,Liu Q. Oxidative coupling and reforming of methane with carbon dioxide using a pulsed microwave plasma under atmospheric pressure. *Energy Fuel*. 2003;17:54–59.
8. Rico VJ,Hueso JL,Cotrino J,Gonzalez-Elipe AR. Evaluation of different dielectric barrier discharge plasma configurations as an alternative technology for green C-1 chemistry in the carbon dioxide reforming of methane and the direct decomposition of methanol. *J Phys Chem A*. 2010;114:4009–4016.
9. Liu CJ,Xue BZ,Eliasson B,He F,Li Y,Xu GH. Methane conversion to higher hydrocarbons in the presence of carbon dioxide using dielectric-barrier discharge plasmas. *Plasma Chem Plasma Process*. 2001;21:301–310.
10. Song HK,Lee H,Choi JW,Na BK. Effect of electrical pulse forms on the CO_2 reforming of methane using atmospheric dielectric barrier discharge. *Plasma Chem Plasma Process*. 2004;24:57–72.
11. Lee H,Lee CH,Choi JW,Song HK. The effect of the electric pulse polarity on CO_2 reforming of CH_4 using dielectric barrier discharge. *Energy Fuel*. 2007;21:23–29.
12. Sekine Y,Yamadera J,Kado S,Matsukata M,Kikuchi E. High-efficiency dry reforming of biomethane directly using pulsed electric discharge at ambient condition. *Energy Fuel*. 2008;22:693–694.
13. Goujard V,Tatibouët J-M,Batiot-Dupeyrat C. Use of a non-thermal plasma for the production of synthesis gas from biogas. *Appl Catal A: Gen*. 2009;353:228–235.
14. Wang Q,Yan BH,Jin Y,Cheng Y. Investigation of dry reforming of methane in a dielectric barrier discharge reactor. *Plasma Chem Plasma Process*. 2009;29:217–228.
15. Rueangjitt N,Akarawitoo C,Sreethawong T,Chavadej S. Reforming of CO_2-containing natural gas using an AC gliding arc system: effect of gas components in natural gas. *Plasma Chem Plasma Process*. 2007;27:559–576.
16. Petitpas G,Rollier JD,Darmon A,Gonzalez-Aguilar J,Metkemeijer R,Fulcheri L. A comparative study of non-thermal plasma assisted reforming technologies. *Int J Hydrogen Energy*. 2007;32:2848–2867.
17. Bo Z,Yan JH,Li XD,Chi Y,Cen KF. Plasma assisted dry methane reforming using gliding arc gas discharge: effect of feed gases proportion. *Int J Hydrogen Energy*. 2008;33:5545–5553.
18. Li XS,Lin CK,Shi C,Xu Y,Wang YN,Zhu AM. Stable kilohertz spark discharges for high-efficiency conversion of methane to hydrogen and acetylene. *J Phys D: Appl Phys*. 2008;41:175203.
19. Li XS,Shi C,Xu Y,Wang KJ,Zhu AM. A process for a high yield of aromatics from the oxygen-free conversion of methane: combining plasma with Ni/HZSM-5 catalysts. *Green Chem*. 2007;9:647–653.
20. Li XS,Shi C,Wang KJ,Zhang XL,Xu Y,Zhu AM. High yield of aromatics from CH_4 in a plasma-followed-by-catalyst (PFC) reactor. *AIChE J*. 2006;52:3321–3324.
21. Ghorbanzadeh AM,Lotfalipour R,Rezaei S. Carbon dioxide reforming of methane at near room temperature in low energy pulsed plasma. *Int J Hydrogen Energy*. 2009;34:293–298.
22. Wang JG,Liu CJ,Eliassion B. Density functional theory study of synthesis of oxygenates and higher hydrocarbons from methane and carbon dioxide using cold plasmas. *Energy Fuel*. 2004;18:148–153.
23. Baulch DL,Cobos CJ,Cox RA,Esser C,Frank P,Just T,Kerr JA,Pilling MJ,Troe J,Walker RW,Warnatz J. Evaluated kinetic data for combustion modelling. *J Phys Chem Ref Data*. 1992;21:411–734.
24. Tully JC. Reactions of $O(^1D)$ with atmospheric molecules. *J Chem Phys*. 1975;62:1893–1898.
25. Tsang W,Hampson RF. Chemical kinetic data base for combustion chemistry. I. Methane and related compounds. *J Phys Chem Ref Data*. 1986;15:1087–1279.
26. Atkinson R,Baulch DL,Cox RA,Hampson JRF,Kerr JA,Troe J. Evaluated kinetic and photochemical data for atmospheric chemistry: supplement IV. IUPAC subcommittee on gas kinetic data evaluation for atmospheric chemistry. *J Phys Chem Ref Data*. 1992;21:1125–1568.
27. Li XS,Zhu AM,Wang KJ,Yong X,Song ZM. Methane conversion to C_2 hydrocarbons and hydrogen in atmospheric non-thermal plasmas generated by different electric discharge techniques. *Catal Today*. 2004;98:617–624.
28. Indarto A,Choi JW,Lee H,Song HK. Effect of additive gases on methane conversion using gliding arc discharge. *Energy*. 2006;31: 2986–2995.

Manuscript received June 23, 2010, and revision received Oct. 3, 2010.